JOURNAL OF GEOPHYSICAL RESEARCH, VOL. 103, NO. D3, PAGES 3381–3397, FEBRUARY 20, 1998

Methods for measuring changes in atmospheric O_2 concentration and their application in southern hemisphere air

Ralph F. Keeling, Andrew C. Manning, and Elizabeth M. McEvoy
Scripps Institution of Oceanography, La Jolla, California

Stephen R. Shertz
National Center for Atmospheric Research, Boulder, Colorado

Abstract. Methods are described for measuring changes in atmospheric O_2 concentration with emphasis on gas handling procedures. Cryogenically dried air samples are collected in 5 L glass flasks at ambient pressure and analyzed against reference gases derived from high-pressure aluminum tanks. Fractionation effects are minimized by avoiding pressure and flow variations throughout the gas-handling system. The overall external reproducibility is approximately ±3.3 per meg, with systematic errors associated with collecting samples and with storing them for 1 year reduced to the level of 3 per meg or smaller. The demonstrated short-term reproducibly of air delivered from high-presure tanks is ±1.5 per meg, with the composition changing by at most 5 per meg by surface desorption reactions as the tank is depleted to below 3500 kPa. A 9-year survey of a suite of six reference gases showed no systematic long-term trends in relative O_2 concentrations to the level of 5 per meg. Results are presented from samples collected at Cape Grim (41°S), Macquarie Island (54°S) and the South Pole Station (90°S). From measurements spanning 1991-1995 it is found that the O_2 concentrations at the South Pole are on average 3.6±1.2 per meg higher than at Cape Grim. This result runs contrary to the expectation that the air at high southern latitudes should be depleted in O_2 as a result of O_2 uptake from the Southern Ocean and may require the existence of unknown O_2 sources near Antarctica or unexpected atmospheric transport patterns.

I. Introduction

Measuring changes in atmospheric O_2 concentration in background air is challenging because the variations occur only at the parts per million (ppm) level relative to the large 21% O_2 background. Over the past decade, two methods with sufficient precision have been developed, one based on interferometry that is used in our laboratory [*Keeling*, 1988a, b] and the other based on mass spectrometry [*Bender et al.*, 1994]. These methods have been used to show that the O_2 concentration varies seasonally throughout the northern and southern hemispheres, is decreasing interannually, and is higher on average in the southern hemisphere than in the northern hemisphere [*Keeling and Shertz*, 1992; *Bender et al.*, 1994; *Keeling et al.*, 1996, 1997]. The O_2 measurements, in combination with measurements of atmospheric CO_2, have made it possible to distinguish oceanic and terrestrial sinks for anthropogenic CO_2 [*Keeling and Shertz*, 1992; *Keeling et al.*, 1993; *Bender et al.*, 1996], to place constraints on biological productivity in the ocean [*Keeling and Shertz*, 1992; *Bender et al.*, 1996], to test models of large-scale oceanic transports [*Stephens et al.*, 1998], and to derive estimates of the large-scale air-sea transfer velocity for O_2 [*Keeling et al.*, 1998].

It is likely that additional O_2 measurement methods (optical and paramagnetic) currently under development in our laboratory and elsewhere will succeed in achieving ppm-level precision or better in the near future. The success of the recently established methods and the geochemical usefulness of the O_2 data have lead to a growth in the number of current or planned measurement programs: at least four programs are under way, and it is likely that additional programs will be initiated in the near future.

Importantly, the development of O_2 sensors of adequate precision only partly addresses the experimental challenge of measuring small changes in O_2 abundance in the atmosphere. Also required are methods for collecting samples and for handling samples and reference gases without altering the O_2 concentration at the ppm level. In our laboratory we have dedicated considerable effort and gained considerable experience in these areas in recent years in conjunction with the atmospheric oxygen measurement program at Scripps. Many of the same experimental issues must be faced by any O_2 program regardless of analysis method, so we expect that

Paper number 97JD02537.
0148-0227/98/97JD-02537$09.00

a description of our methods and experiences will benefit the O_2 measurement community as a whole. Such a description is the primary purpose of this paper.

Changes in O_2 concentration can conveniently be expressed in terms of changes in the O_2/N_2 ratio according to

$$\delta(O_2/N_2) = \frac{(O_2/N_2)_{sample}}{(O_2/N_2)_{reference}} - 1 \qquad (1)$$

where $\delta(O_2/N_2)$ is typically multiplied by 10^6. We refer to such parts per million changes in a ratio as "per meg" units. As clarified below, 4.8 per meg units are essentially equivalent to 1 ppm (i.e. 1 μmole O_2 per mole of dry air).

The need to measure very small changes in the relative abundance of a major constituent of air raises a number of unique gas-handling issues. One such issue is the need to avoid diffusive separation of O_2 and N_2 induced by temperature, pressure, or water vapor gradients which lead to the preferential accumulation of O_2 in regions with lower temperatures, higher pressures, or higher absolute humidities, respectively [*Chapman and Cowling*, 1970; *Severinghaus et al.*, 1996]. Fractionation by pressure gradients occurs not only for hydrostatic pressure gradients induced by gravity but also for flow-related pressure gradients. The potential degree of fractionation can be calculated for conditions under which molecular diffusion is the only gas transport mechanism. As outlined in Table 1, the potential fractionations are very large compared with variations in background air, falling in the range of 1000 to 10000 per meg for typical temperature, pressure, or moisture gradients encountered in sample handling. If macroscopic flow also contributes to gas transport, as is inevitable in the case of flow-related pressure gradients, the actual degree of fractionation will be smaller by a factor related to the timescale for diffusive transport divided by the timescale for turbulent mixing or advective replacement of the air sample. Taking a diffusivity of 0.2 $cm^2\ s^{-1}$, a length scale of 10 cm, and a flow velocity of 100 $cm\ s^{-1}$ yields a reduction factor of the order of (10)(100)/(0.2) = 5000. Of course, circumstances will vary, and this suggests that while appropriate gas-handling strategies can reduce the fractionation to levels of 1 per meg or less, the potential exists for large artifacts unless care is taken.

Another potential fractionation mechanism involves flow through any orifice with a characteristic diameter smaller than the mean-free path between molecular collisions. Here the governing transport mechanism is Knudsen diffusion whereby the molecular flow is proportional to the partial pressure differential and the molecular velocity, which varies inversely with the square-root of the molecular weight [*Dushman*, 1962]. The ratio of the O_2 to N_2 flows through an orifice with a large pressure drop is thus $(28/32)^{1/2} = 0.946$ times smaller than the abundance ratio upstream of the orifice. For example, a small leak which leads to a loss of only 0.1% of a sample can potentially enrich the O_2/N_2 ratio of the remaining sample by as much as $(1\text{-}0.946)(0.01)(10^{-6}) = 64$ per meg by this mechanism.

Finally, fractionation can occur due to adsorption of O_2 and N_2 onto solid surfaces or due to the dissolution of these gases into permeable solids, such as elastomeric seals. For example, a 1 L sphere holds 0.044 moles of gas at 1 atmosphere STP, while a one monolayer coverage of the sphere's surface holds roughly 10^{-4} moles or 2×10^{-5} of the gas phase abundance. Most real surfaces are very rough on the molecular scale and so effectively have the capacity for adsorbing many monolayers although these capacities are often hard to quantify. For reversible physisorption, the amount adsorbed typically increases with pressure, with a different effective partition coefficient for different gases. Thus one detectible manifestation of physisorption is changes in the gas phase abundance associated with pressure changes in the vessel. Such changes can easily occur at the level of 10 per meg or higher. Adsorption can also be irreversible, as for oxidative chemisorption of O_2.

The strategy we have adopted for minimizing gas phase and surface fractionation processes, as described below, involves exposing air samples and reference gases to pressure, temperature, or moisture gradients only under conditions of steady flow. Mass balance thus ensures that the relative flows of O_2 and N_2 into any region must equal the relative flows out of the region even if concentration gradients due to

Table 1. Diffusive Fractionation Mechanisms

Fractionating Process	Linearized Equations[a]	Example Calculation
Thermal Diffusion	$\delta = -\alpha\,\Delta T/T$	$-(0.018)(20/298)(10^6) = -1208$ per meg[b]
Pressure Gradient	$\delta = \frac{(m_{O_2} - m_{N_2})}{m_{air}}\,\Delta P/P$	$\frac{(32.-28.)}{(29.0)}(0.1/1.0)(10^6) = 13800$ per meg[c]
Water Vapor Diffusion	$\delta = \left(\frac{D_{N_2,H_2O}}{D_{O_2,H_2O}} - 1\right)\Delta X_{H_2O}$	$(0.965\text{-}1)(0.03)(10^6) = -1050$ per meg[d]

[a]Valid for small gradients in temperature, pressure, or humidity.

[b]Based on thermal diffusion coefficient for O_2 and N_2 of $\alpha = 0.018$ [*Grew and Ibbs*, 1952] and based on an assumed 20°C temperature gradient.

[c]Based on an assumed 10% gradient in absolute pressure.

[d]Based on the diffusivity ratio of 0.965 [*Severinghaus et al.*, 1996] and a gradient in water vapor mole fraction ΔX_{H_2O} equal to the difference between dry air and air saturated at 1 atmosphere pressure and 25°C.

moisture, pressure, or temperature gradients exist within the region itself. By maintaining constant flows, we additionally maintain constant pressures and thereby reduce the potential for fractionation induced by surface adsorption or desorption.

A related issue is the need for establishing a stable long-term reference for quantifying the long-term trend in atmospheric O_2 abundance. Since the geochemically interesting questions depend only on measuring relative changes, a suitable reference material would be any air-like mixture of N_2, O_2, Ar, plus trace gases that can be handled reproducibly over the short term to the level of a few per meg in O_2/N_2 and can be demonstrated to be stable over several decades to the level of about 5 per meg [*Keeling et al.*, 1993]. At the outset we faced the difficulty that standards for O_2 in air of sufficient accuracy were not available. Even more fundamentally, we faced the difficulty that the question of how to handle reference gases at the required level of reproducibility was totally unexplored. For these reasons we had no alternative but to focus our efforts on short-term gas-handling strategies and accept the risk that our reference gases, which consist of compressed air stored in various types of high-pressure tanks, might not be stable over the long term. Our discussions here focus mainly on issues involving short-term gas handling. Nevertheless, we will also present data on the relative stability of our reference gases that indicate a high level of stability over many years.

The remainder of this paper is organized as follows: Section 2 presents a review of the general relationships between the instrument responses and the changes in O_2 concentration and discusses relationships between different units for reporting changes in O_2 abundance. Section 3 presents a description of the apparatus and procedures for analyzing flask samples and for preparing and intercomparing reference gases. Section 4 describes our methods for establishing calibration factors and describes the tests we have conducted to assess the long-term stability of our reference gases. Section 5 describes apparatus and procedures used to collect air samples in glass flasks, describes tests demonstrating that reliable samples can be collected and stored for periods approaching 1 year, and describes the flask-to-flask reproducibility that we achieve. Section 6 presents an example of our data illustrating a small north-south gradient detected between two stations in the southern hemisphere. The geochemical significance of this gradient is discussed in relation to potential sampling biases. Finally, section 7 summarizes our primary findings.

2. Reporting O_2 Concentrations

Oxygen concentrations are determined in our laboratory using an interferometric method based on changes in the relative refractivity of air. Small changes in relative refractivity are related to air composition according to

$$\delta r = \sum_i S_i \delta X_i \qquad (2)$$

where δr is the change in the relative refractivity, S_i is a coefficient that expresses the sensitivity of the relative refractivity to changes in constituent i [*Keeling*, 1988a], and δX_i is the difference in the mole fraction of constituent i relative to an arbitrary reference. The change in relative refractivity δr is directly proportional to the interferometrically observed changes in a fringe remainder (see Appendix A). The sensitivity relationship for the interferometric method is thus of a general form involving a linear relationship between changes in mole fractions and the instrumental response. Further details of the interferometric method are given in Appendix A and by *Keeling* [1988a, b].

One conceptual complication with eq (1) is that the mole fractions of different constituents are not independent insofar as the addition or removal of a particular constituent changes not only the mole fraction of that constituent but also the mole fractions of every other constituent by dilution. The dilution effects due to water vapor, the most variable component of air, can be eliminated by drying the air, which is routinely done in our laboratory for all samples. Residual dilution effects, for example due to addition or removal of CO_2, have a negligible effect on the mole fractions of trace gases, but they produce nonnegligible changes in the mole fraction of O_2. To avoid dilution effects on O_2, we express the O_2 mole fraction on a basis free of H_2O, CO_2 and other trace gases, and we use the appropriate sensitivity coefficient S_{O_2} for this basis.

With this convention we can solve eq (2) for the difference in O_2 mole fraction between a sample and a reference according to

$$\begin{aligned}\delta X_{O_2} &= X_{O_2}^{(\text{samp})} - X_{O_2}^{(\text{ref})} \\ &= S_{O_2}^{-1}\left(\delta r - \sum_{i \neq O_2} S_i (X_i^{(\text{samp})} - X_i^{(\text{ref})})\right)\end{aligned} \qquad (3)$$

where the summation takes into account interferences from trace gases on the instrument response. In principle, the determination of changes in O_2 mole fraction requires an independent method for determining changes in the abundance of all trace gases. In practice, the only large interferences in H_2O-free background air using the interferometric method are due to CO_2.

Our procedures thus yield via eq (3) the change in the O_2 mole fraction on a CO_2-free basis relative to a reference gas. We alert the reader that this method of reporting changes in O_2 concentration, while seemingly conceptually clear, can cause confusion in a geochemical context. Consider an air sample containing one million molecules, of which 209500 are O_2 and 350 are CO_2. Adding one molecule of O_2 to the sample increases the number of O_2 molecules to 209501 and the total number of molecules to 1000001, so that the O_2 mole fraction increases by 0.79 μmole mole^{-1}. The change in O_2 mole fraction is essentially the same whether we consider the mole fraction on a basis with or without CO_2. In comparison, adding one molecule of CO_2 to the sample increases the number of molecules of CO_2 to 351 and increases the CO_2 mole fraction by 0.9996 μmole mole^{-1}, which is virtually equal to 1 μmole mole^{-1} because the percent increase in the total number of molecules is much smaller than the percent increase in CO_2. The addition of CO_2 decreases the O_2 mole fraction by 0.21 μmole mole^{-1} on a basis containing CO_2. While reporting O_2 changes on a CO_2-free basis eliminates the sensitivity of

the O_2 mole fraction to CO_2 exchanges, the CO_2-free basis still leads to confusion because a change involving the same number of molecules leads to a smaller change in the O_2 mole fraction than in the CO_2 mole fraction.

Largely to avoid this source of confusion, we have adopted the practice in our laboratory of expressing changes in O_2 abundance in terms of changes in the O_2/N_2 ratio. This approach is also advantageous in allowing our results to be directly compared with results of other laboratories that employ the mass spectrometric method, in which the O_2/N_2 ratio is the directly observed quantity [*Bender et al*, 1994]. Assuming that the relative abundances of N_2, Ar, and other inert gases are constant, it can be shown that changes in O_2/N_2 ratio (relative to a real air reference) are related to the changes in mole fraction (relative to the same reference) according to

$$\delta(O_2/N_2) = \frac{\delta X_{O_2}}{(1 - X_{O_2})X_{O_2}} \quad (4)$$

Here X_{O_2} represents the O_2 mole fraction on a CO_2-free basis, which we can approximate by the constant value of 0.2095 [*Machta and Hughes*, 1970]. Although the assumption of constant relative abundances of N_2 and the inert gases cannot be strictly valid, the errors in eq (4) which result from natural variations in background air can easily be shown to be negligible.

It may be useful to illustrate how the change in O_2/N_2 ratio is computed for transformation in which one molecule of O_2 is added to the air sample containing a 209500 O_2 molecules out of a total of 1000000. The increase in O_2 abundance relative to the initial O_2 amount is $1/209500 = 4.8 \times 10^{-6}$. Since N_2 is constant, the relative change in the O_2/N_2 ratio is also equal to 4.8×10^{-6} or 4.8 per meg. This shows that 4.8 per meg is equivalent to the same number of molecules as 1 μmole mole^{-1} in a trace gas abundance. It is in this sense that 4.8 per meg is equivalent to 1 ppm (i.e., 1 μmole mole^{-1}).

3. Laboratory Gas Handling

3.1. Apparatus

The apparatus we use for analyzing flask samples and for comparing their concentrations to reference gases is shown in Figure 1. The apparatus allows alternatively a working gas or reference gases to be directed through lines which pass serially through a CO_2 analyzer and then through the interferometeric O_2 analyzer. Flasks are analyzed, as described further below, by optionally diverting the flow through the flasks. Pressures are actively stabilized at three locations: a point upstream of the flask, at the CO_2 analyzer, and a point upstream of the oxygen analyzer. Sensitive pressure control is achieved at the CO_2 and O_2 analyzers by the use of sensitive differential gages referenced to the pressure in thermally insulated, sealed volumes. During reference gas comparisons and flasks analysis, the CO_2 analyzer output voltage, the output of the interferometric O_2 analyzer (fringe remainder), and the system flow rate are simultaneously logged on a computer system and displayed on a strip chart recorder.

3.2. Flask Analysis Procedures

Our air samples are collected in 5 L flasks filled with dried ambient air at approximately 1 atmosphere pressure, as described in section 5 below. Before each analysis, a small magnetic (ALNICO) stir bar is inserted into the flask. During analysis the stir bar is rotated with a magnetic stir base to ensure that the air in the flask is mechanically mixed, thus yielding a more reproducible "sweep-out" curve during analysis and reducing any possible concentration gradients within the flask resulting from thermal diffusion.

The analysis procedure involves flushing out the contents of each flask with flow of working gas. This method was adopted in order to reduce pressure and flow perturbations in the interferometer cell, the flask, and the intervening lines during analysis. The working gas is prepared to have an O_2/N_2 ratio and CO_2 mole fraction close to the annual-mean atmospheric values. The working gas initially bypasses the flask (valve *o* opened, both flask stopcocks closed; see Figure 1), but during analysis, it is directed through the flask (*o* closed, stopcocks opened). During the analysis the chart pen traces consist of transient deflections away from the steady reading of the working gas followed by a quasi-exponential decay back toward the working-gas reading. After 10 min of analysis the flow is diverted around the flask (*o* opened, stopcocks closed) to reestablish the working-gas baseline. The maximum deflection on the "sweep-out" curve relative to the working gas reading is determined by hand-ruling the chart. This peak deflection is proportional to the difference in composition between the flask sample and the working gas. The peak deflection depends both on the span sensitivity of the CO_2 and O_2 analyzers and on correction factors which account for the degree to which the flask air is diluted with working gas during analysis. Section 4 describes how these calibration factors are derived.

3.3. Tank Intercomparison Procedures

Reference gases derived from compressed air tanks are intercompared by using the following procedures prior to analysis: (1) tanks are stored horizontally in the insulated enclosure for at least 10 hours; (2) the high-pressure lines are pressurized and vented at least 3 times before they are left open to the tank; (3) the high-pressure lines are left open to the tank pressure for at least 2 hours, and (4) the high-pressure lines, still at tank pressure, are fully swept out with gas. The first two steps are precautionary, to ensure tanks are isothermal and to eliminate room air from the high-pressure lines. The last two steps were adopted after we found that the gas initially derived from tanks is detectably depleted in O_2 and CO_2. Most likely, this transient depletion is caused by selective adsorption of O_2 and CO_2 on surfaces newly exposed to high pressures; we suspect this adsorption may be linked to the desorption of water vapor. We also found that the initial depletion is larger when the tank pressure is higher and when stainless steel fittings and tubing are used. The rate of uptake is greatly reduced after several hours of conditioning at tank pressure. We now scrupulously avoid

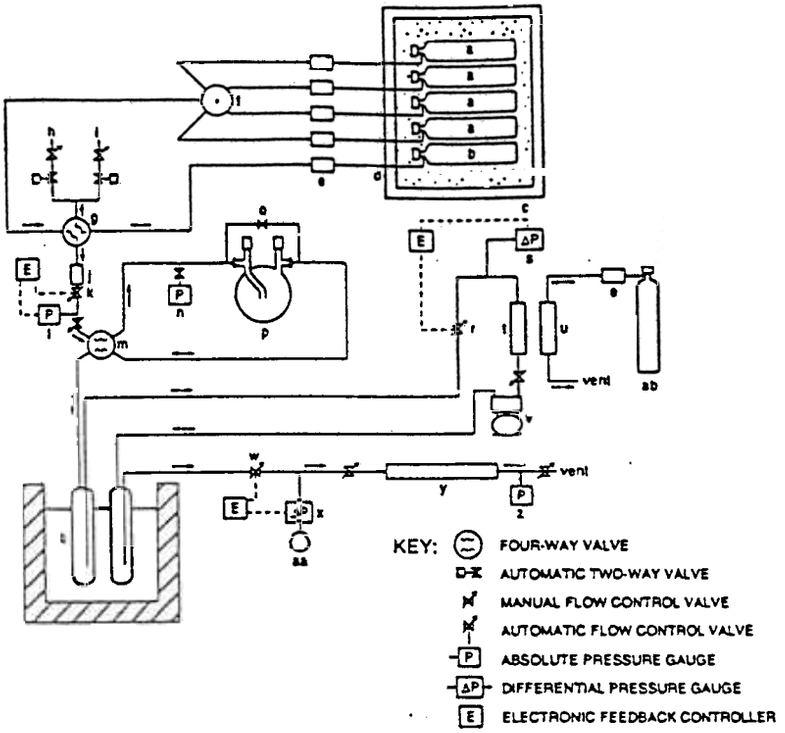

Figure 1. Gas-handling system for atmospheric O_2 measurements used for reference gas calibration and flask analysis: a, reference tanks, oriented horizontally; b, working tank, oriented horizontally; c, insulated enclosure, d, high-pressure lines (1/16" OD nickel); e, gas regulators set to an outlet gage pressure of ~172 kPa (10 PSIG); f, 16-port valve (Valco Instr., for simplicity, a four-port valve is shown); g, automatic four-way valve; h and i, tank purge ports; j, electronic flow meter; k, automatic flow-control valve (MKS Instr., 248); l, absolute pressure gage (MKS, 122); m, manual four-way valve; n, absolute pressure gage used intermittently; o, flask bypass valve; p, sample flask; q, stainless-steel cold traps packed with glass beads in a cold bath at -80°C; r, automatic flow-control valve (MKS, 248); s, differential pressure gage with full-scale sensitivity of ±10 torr (MKS, 223B); t and u, CO_2 analyzer (Siemens Ultramatt 3) sample and reference cells, respectively; v, diaphragm compressor (Neuberger, N05); w, automatic flow-control valve (MKS, 248); x, differential pressure gage with full-scale sensitivity of ±10 inches of water (Sensotec, Z890-20); y, interferometer sample cell; z, absolute pressure gage; aa, thermally insulated static volume serving as reference pressure at ~240 kPa; ab, CO_2-in-air reference tank with nominal concentration of 320 μmole mole^{-1}. Most gas lines used are chemically cleaned (Process C, Tube Service Company) 1/8" OD 316 L stainless steel. The figure shows the apparatus used in Boulder, Colorado, where ambient pressure is typically 816 mbar. After being moved in 1993 to La Jolla, California, where ambient pressure is typically ~1000 mbar, the apparatus was modified by connecting the reference port of the differential pressure gage (s) and the exhaust line of the CO_2 analyzer reference cell (u) to a dynamic stream of room air actively stabilized at 816 mbar. This served to maintain equal pressures of 816 mbar in the two CO_2 analyzer cells (t and u), independent of ambient pressure.

using stainless steel for any surfaces exposed to tank pressures, using instead unplated brass, chrome-plated brass, or nickel.

Reference gases are generally compared 3 times against the working gas in a sequence WAWAWA-WBWBWB- etc., where each letter represents 10 min of analysis, with W representing the working gas and A and B representing different reference gases, and where the dashes mark the times when the multiport valve (f) is switched. During the 10 min before a new reference gas is introduced, this reference gas is exhausted into the room via the four-way valve (g) at a flow rate of approximately 5 STP cm^3 s^{-1}. This "fast purge" is used to sweep the lines and regulators free of stagnant gas that has been stored in the lines and may be depleted in O_2 and CO_2, as described above. At all other times during the analysis sequence, the gas that is not selected by the four-way valve (either the working gas or the selected reference gas) is exhausted into the room at a flow rate of approximately 0.8 STP cm^3 s^{-1}. This "slow purge" is used to prevent O_2 or CO_2 depletion from occurring in the otherwise static line. We do this because we have seen evidence that very low levels of depletion continue for hours and perhaps days. This apparently inexhaustible depletion process is probably caused by a different mechanism, perhaps involving selective permeation of O_2 through O-rings in the regulators.

The concentration difference between the reference tank and the working tank are computed 3 times for the

WAWAWA-W sequence based on the average of the forward and backward differences. We generally reject the first of these three analyses, because we have found from looking at many tank comparisons that the first analysis yields O_2/N_2 values for the reference tank which are low by 1 to 2 per meg compared with the two following analyses: We suspect that even with our precautions the first analysis is still detectably influenced by residual surface reactions in the high-pressure lines and fittings. The precision obtained by averaging the second and third transitions is approximately ±1 per meg.

We have tested for fractionation within the tank delivery lines by connecting two delivery lines to a single tank. This we accomplished with a high-pressure "*T*" which allows two regulators to be connected to one tank. By following the same procedures as above but now comparing a tank against itself, we achieve a sensitive measure of any concentration differences caused by differences in lines or regulators. These tests showed that our procedures reduce any such differences to below 1 per meg. Incidentally, our initial attempts to demonstrate this consistency using a "*T*" constructed from stainless steel pipe fittings were unsuccessful. The successful demonstration required using a "*T*" constructed from a monolithic block of brass. Reducing thermal gradients in the "*T*" appeared to be crucial.

3.4. Gas Tanks and Filling Procedures

Reference and working tanks are filled by using an oil-free compressor (RIX Industries). The compressed air is purified and dried to below 5 μmole mole^{-1} of H_2O using a cartridge filled with type 13X molecular sieve. Using molecular sieves, which tend to remove CO_2 and can alter O_2/N_2 ratios, is acceptable because our procedures do not require that the reference gases contain "real" air samples. Tank concentrations are adjusted to the desired CO_2 concentration or O_2/N_2 ratio by pumping in additional amounts of pure CO_2, N_2, or O_2.

For the first few years of our program we used working tanks and secondary reference gases made of either aluminum or chrome-molybdenum steel. More recently, we have been using exclusively aluminum tanks, which tend to exhibit better short-term stability, as described below. Our six primary reference tanks are all aluminum (Luxfur) tanks treated with the proprietary Airco "Spectra-Seal" surface treatment on the inside. Further specifications of the primary reference tanks are summarized in Table 2.

4. Instrument Calibration

4.1. Span Calibration

The differential sensitivity of the interferometer output to changes in O_2 concentration, i.e., the span sensitivity, is based on the sensitivity factors which are derived as described in Appendix A. As a cross-check on the span calibration, we also prepared gravimetric standard mixtures of N_2, O_2, Ar, and CO_2 in small high-pressure tanks and then measured the differences in O_2 concentration between these standard mixtures using the interferometer after correcting for differences in trace gas and inert gas abundances. The linear regression between the O_2 mole fractions in the tanks determined from the gravimetric data versus the mole fraction determined from interferometric measurements yielded a slope of 0.996±0.007 which confirms our span calibration to better than 1%. Details of the methods used to prepare the gravimetric standards will be described elsewhere.

We have also confirmed the CO_2 sensitivity coefficient needed for computing the CO_2 interference by bleeding variable amounts of CO_2 into an airstream derived from a high-pressure tank and recording the relative refractivity changes on the interferometer while simultaneously recording the CO_2 changes using the infrared CO_2 analyzer. These tests confirmed that the CO_2 sensitivity coefficient (see Table 3, Appendix A) is also valid to better than 1%.

An additional span calibration factor is needed to correct for the dilution of flask air with working gas during flask analysis. This factor depends slightly on flask fill pressure. We determined this dilution factor by preparing flasks with known concentration differences from the working tank and comparing the actual peak heights with the heights expected for zero dilution. This comparison was done at a range of flask pressures. We then apply this correction factor to analyzed flasks, after determining the flask pressure from the magnitude of the small flow perturbations that occur during analysis. We accept flasks if their pressures fall in the range between 920 and 1090 mbar. Over this range the dilution factor varies from 0.85 to 0.93 for the O_2 measurement.

4.2. "Zero" Calibration

We establish a "zero" or reference point for the atmospheric oxygen concentration using a hierarchical strategy in which

Table 2. Primary Reference Tanks

Tank ID	Internal Volume, liters	Internal Surface Area, cm^2	Pressure, kPa	
			Oct. 1990	Nov. 1994
43230	29	7200	10300	9400
43418	29	7200	9700	8600
5178	47	9200	9900	7600
6999	47	9200	12800	12300
7014	47	9200	4700	4300
7017	47	9200	7200	5400

the working gas (against which all flasks are analyzed) is compared against a pair of secondary reference gases on every day that flasks are analyzed, and these secondary reference gases, in turn, are calibrated against a set of six primary reference gases at approximately 6 month intervals. This strategy is designed to provide redundant information useful for assessing the stability of the reference point on both short and long timescales.

Every day that flasks are analyzed, a daily working tank concentration is derived by adding the observed difference between the working tank and the two secondary reference tanks to the previously established concentrations of the secondary reference tanks. This comparison with the two reference gases yields two independent estimates of the working tank concentration, and these two numbers are averaged to yield the daily value assigned to the working tank. Preliminary flask concentrations are assigned by adding the flask-working tank differences (corrected for dilution on analysis) to these working tank concentrations. We refer to these preliminary concentrations as being on the "S1" scale.

At approximately 6 month intervals we run six primary reference gases against the working tank. Primary reference tanks are typically analyzed in a sequence a-b-1-2-3-4-5-6-a-b, where "a-" and "b-" denote hour-long comparisons of secondary reference gases A and B, respectively, with the working tank (i.e., "a-" denotes WAWAWA-), and where "1", "2"..., denote hour-long comparisons of primary reference gas 1, 2, etc., against the working tank. As for flask analyses, the comparisons with the secondary reference gases are used to compute "S1" values for the working gas, and this value is added to the difference between each primary reference gas and the working gas to yield the preliminary (i.e., "S1") concentrations of the primary reference gases.

Working tanks usually last 3 to 6 months, and we replace them when their pressure drops to between 1600 and 800 kPa. The secondary reference gases last approximately 2 years, and we replace them when their pressure drops to about 3300 kPa. New secondary reference gases are brought into use only after they have been analyzed repeatedly over a period of several months against the "S1" scale using the same procedure as for the primary reference gases. The history of the "S1" values on these new tanks is used to assign a permanent "S1" value to the tank. After this tank is brought into use as a secondary reference tank, its assigned "S1" value never changes. Replacements of the working tanks and secondary reference tanks are staggered so that only one of the three tanks is replaced at a time. These procedures allow the "S1" scale to be propagated indefinitely into the future.

We expect that the zero of the "S1" scale may slowly drift in absolute terms for a variety of reasons, including drift in the secondary reference gas composition or small random errors in their initial assigned concentrations. Our strategy for correcting for this drift involves examining the overall history of the six primary reference gas concentrations and applying a time-varying additive correction function to their "S1" values to bring the primary reference gas concentrations back to constant values. A single correction function is applied to all primary reference gases. We refer to the corrected scale as the final or "S2" scale. The "S2" values may be subject to revision as more or better information on tank drift becomes available. The "S2" and "S1" scales are arbitrarily defined to coincide in October 1990 and to yield a value of zero for a particular primary reference gas (tank 7017) at that time.

Flasks concentrations, initially assigned on the "S1" scale, are also corrected to the "S2" scale using the same additive corrections. Our methods for calibrating CO_2 measurements closely follow the procedures for oxygen and are described in Appendix B.

4.3. Stability Cross-Checks

A cross-check on the short-term stability of our calibration procedures is provided by the daily "S1" value of the working gas, which as discussed above, is redetermined independently each day that flasks or reference gases are analyzed. We initially used mostly chrome-molybdenum steel tanks as working tanks for which the standard deviation of the daily "S1" values relative to the tank average varied from ±1.8 to ±7.7 per meg, depending on the tank. More recently, we have used exclusively aluminum tanks, and the same figures for the aluminum tanks range from ±1.4 to ±2.2 per meg as shown in Figure 2. These variations include a seemingly random component with a variability of around ±1.4 per meg, plus possible longer-term systematic trends.

The magnitude of any long-term trends place constraints on the magnitude of any concentration changes induced by desorption from the tank walls as the tanks are depleted. While apparently significant trends are evident for three of the six working tank histories shown in Figure 2, these trends are no larger than 5 per meg for pressures above 3300 kPa. This result is significant because it largely eliminates concerns regarding desorption effects for our primary reference gases, which have suffered less depletion than the working tanks.

Additional information on the long-term stability of the primary reference tanks is provided by their relative differences over time. The values of the primary reference tanks on the "S2" scale are shown in Figure 3 along with the corrections applied to eliminate the assumed drift of the "S1" scale. Stepwise corrections were applied in 1991 in association with well-documented changes in the thermal environment of the secondary reference tanks. Since June 1991, when the secondaries were first loaded into the insulated enclosure, essentially no corrections have been applied other than allowing for a slight upward drift in 1992-1993. The corrections eliminate most of the long-term drift in these tanks except for a general upward shift in the middle of 1992.

We have not attempted to correct for the 1992 shift because we believe it reflects a real change in the composition of the primary reference tanks associated with their being transferred from a vertical position in the laboratory to a horizontal position in the insulated enclosure. Our reasoning is as follows: The six primary tanks were moved into the enclosure two-at-a-time over a period of several months in 1992 with analyses performed at each step. Compared to the long-term history of the concentration difference between these tanks, we found a consistent shift of about 10 per meg in the tanks moved into the enclosure relative to tanks remaining outside,

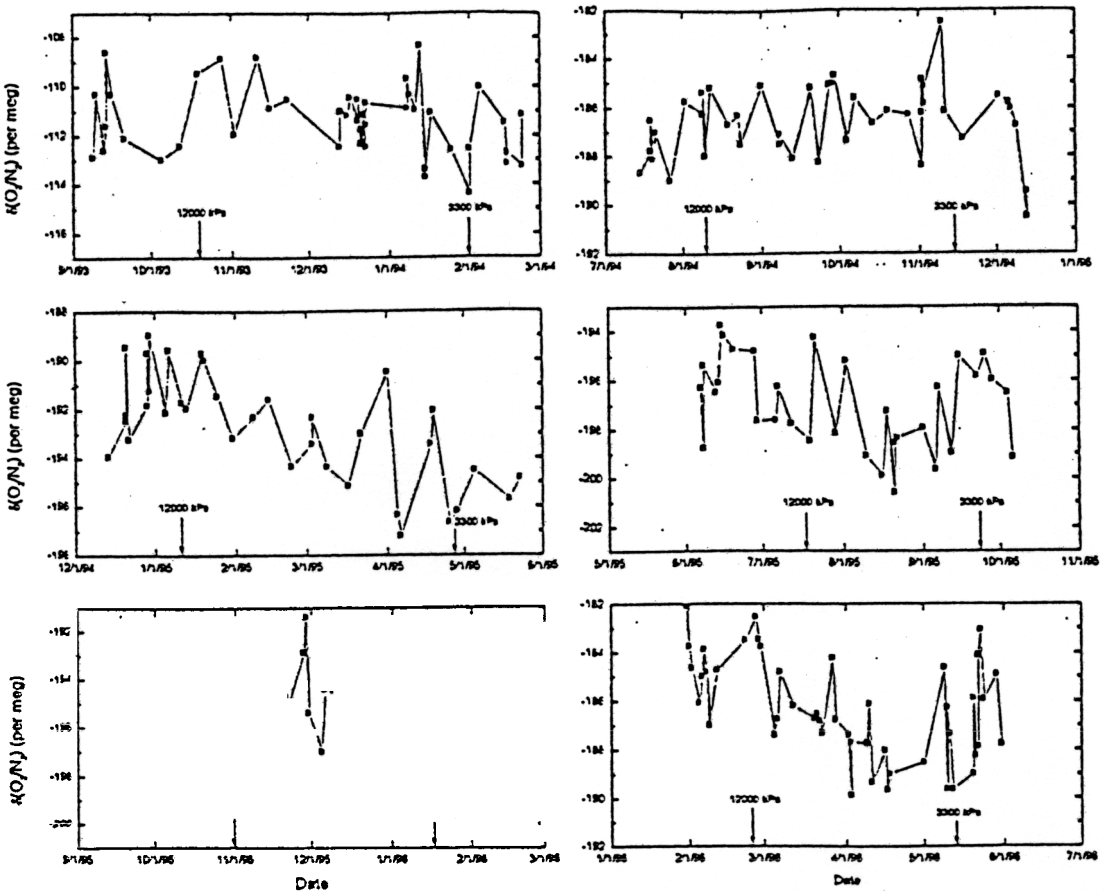

Figure 2. O_2 concentrations of the air derived from six aluminum working tanks over their full usage history. The concentrations are determined as described in the text and are effectively expressed on the "S1" scale without corrections for CO_2 interferences. Also shown are the times at which the tank pressure equaled 12000 kPa and 3300 kPa.

as shown in Figure 4. This shift seen in the pairwise differences is very nearly the same magnitude as the apparent shift in the primaries against the "S1" scale during 1992, thus suggesting that the tanks really increased their concentrations by about 10 per meg. Consistent with this interpretation is the fact that we also observed an apparent shift of the opposite sign when the secondaries were moved into the enclosure in 1991 (event *iii*, Figure 3), while the primaries remained outside.

The upward shifts in reference gas composition that occurred when the tanks were moved into the enclosure could have been caused either by thermal or by gravimetric (i.e., pressure induced) fractionation in the tanks. At barometric equilibrium the O_2/N_2 ratio at the top of a tank 1 m in height would be 17 per meg lower than the ratio at the bottom. The gradient is the right order of magnitude and sign to explain the shift. However, the time required to achieve such a gradient is of the order of 1 year, given the slow diffusion at high pressures. Thermal diffusion could lead to concentration gradients over shorter length scales and timescales and thus seems a more likely cause of the upward shifts.

Other than the parallel upward excursion of all the tanks in 1992, we see little evidence for any long-term changes in the primary reference gas composition. The relative stability of the primary reference tanks is excellent; any such drift has been at the level of ±5 per meg or smaller over the full 9 to 10-year history of these tanks, as shown in Figure 4.

5. Flask Sampling

5.1. Sampling Methods

Our air samples are collected in 5 L spherical glass (Pyrex) flasks which are equipped with a pair of stopcocks, one with an injector tube, to allow flushing with sample air. The stopcocks (supplied by J. Young Scientific Glassware) have glass pistons and Viton O-rings which we lubricate with small amounts of Apiezon type N grease. We also tested, but later abandoned, the use of Teflon O-rings after problems with long-term sample storage became apparent. The flask volume of 5 L is determined by the need for sufficient sample to fill the interferometer cell during analysis. Flasks are delivered to the collection sites containing dry air at 1 bar. At each site, the flasks are flushed thoroughly with dried ambient air at a constant pressure of 1 bar which is delivered by a pumping module (Figure 5). The flasks are flushed at flows of 2 to 5 STP L/min and the air is passed through a cold trap at temperatures ranging from -55°C to -90°C, depending on

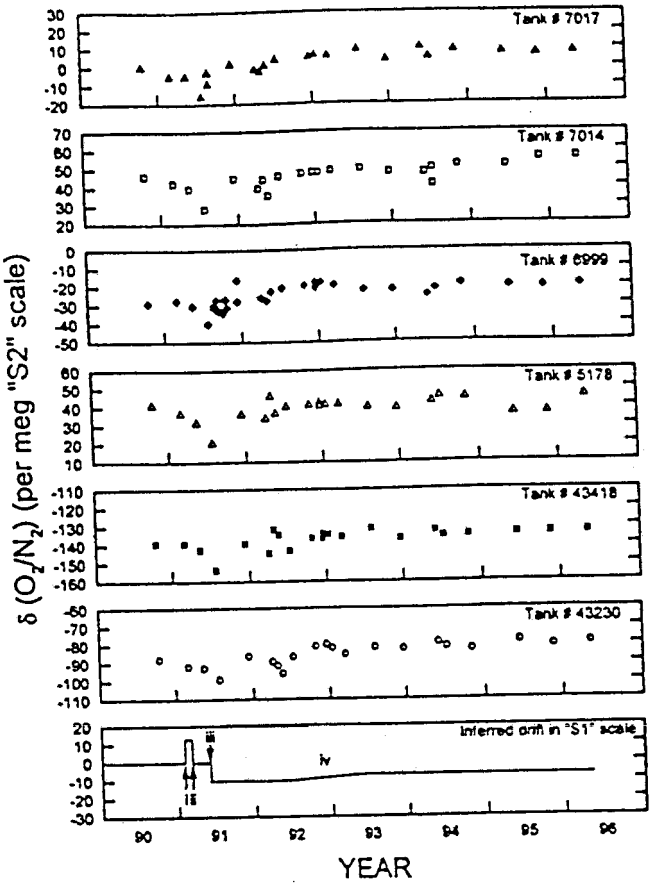

Figure 3. Histories of the O_2/N_2 ratios of the six primary reference gases relative to the final (S2) scale and corrected for CO_2 interference. The bottom panel shows the corrections (subtractive) applied to the preliminary (S1) scale in order to compute final values on each reference tank. The same corrections are applied to each primary reference tank. Event i, secondaries placed near a laboratory heat source (chiller unit); event ii, secondaries moved away from laboratory heat source; event iii, secondaries oriented horizontally in the insulated enclosure; event iv, allowing for possible slow drift of unknown cause in secondaries. A noticeable upward shift of 5 to 10 per meg is evident near the middle of 1992 for all six reference gases. We believe this shift reflects a real change in the composition of the tanks caused by their relocation to a horizontal position in the insulated enclosure. The laboratory was moved from Boulder, Colorado, to La Jolla, California, between January and March 1993. No corrections were needed for this move.

the site, to remove water vapor. We also tested collecting flasks dried only to a dew point of 0°C but found that this lead to problems during analysis. Whether high dew points also cause problems intrinsic to collection or storage of samples is not clear.

The apparatus is typically located indoors in a remote building at the field site, with the intake line running outdoors and up a tower to the windward side of the building. Sampling indoors reduces the magnitude of possible temperature gradients around the flasks, which could lead to artifacts resulting from thermal diffusion within the flasks. Depending on the site, flasks are either flushed individually, as shown in Figure 5, or flushed three-at-a-time in series.

5.2. Flask Sampling Tests

We have tested our flask-sampling procedures by comparing air samples collected in flasks with direct measurements of the O_2 content in air. Eight flask samples were collected at La Jolla, California, under conditions of steady ambient O_2 readings, while the air was simultaneously monitored with the interferometer using a continuous analysis method [*Keeling*, 1988b]. Samples were subsequently analyzed against the same reference gases used to calibrate the ambient measurements. Expressed relative to ambient air, the O_2/N_2 ratios of seven of the flasks had a mean value of +1.8 per meg and a standard deviation of ±2 per meg. This suggests that our sampling procedures are reliable to ±2 per meg, which is about as well as we can guarantee short-term stability of our calibration. We have no explanation for the results from the eighth flask (-28 per meg), which was an obvious outlier.

5.3. Flask Stability Tests

We have tested the stability of O_2/N_2 ratios and CO_2 concentrations in our flasks by setting aside six flasks and analyzing their concentrations over time. In order to amplify possible sources of instability, we inserted 20 ungreased Viton O-rings into one pair of flasks and 20 greased O-rings into another pair. These O-rings were in addition to the pair used on the seats of the stopcocks. The final pair of flasks contained only dry air, like our normal flasks. All O-rings were used here as provided by the manufacturer without baking. After inserting the O-rings, we flushed these flasks thoroughly at atmospheric pressure with air derived from a particular high-pressure tank and stored the flasks in the dark in boxes kept in the laboratory. Periodically over the next year, the flasks were analyzed by using the same high-pressure tank for the working gas.

The concentration trajectories of these flasks relative to air delivered from the high-pressure tank are shown in Figure 6. In calculating these trajectories we have corrected for the complication that our analysis procedure alters the composition in the flasks by diluting the flask air with tank air. We corrected for this alteration based on the fraction of the air in the flasks which is replaced during each analysis, so the results in Figure 6 essentially show the trends that would have occurred had no dilution occurred. All flasks, including those without extra O-rings or grease, show an apparent downward drift in O_2/N_2 between the day of flushing (day 0) and the first day of analysis (day 4). We believe these shifts are at least partly due to changes in the composition of the air delivered from the high-pressure tank, and we therefore consider only the changes that occured after day 4 to be significant. (The O_2 concentration delivered from the tank may have varied with delivery flow, yielding higher O_2 concentrations during the initial flask purging, when much higher flows were used.)

It appears that there are at least two processes occurring in the flasks with extra O-rings. The first process is indicated by the simultaneous decreases in both O_2/N_2 and CO_2 over

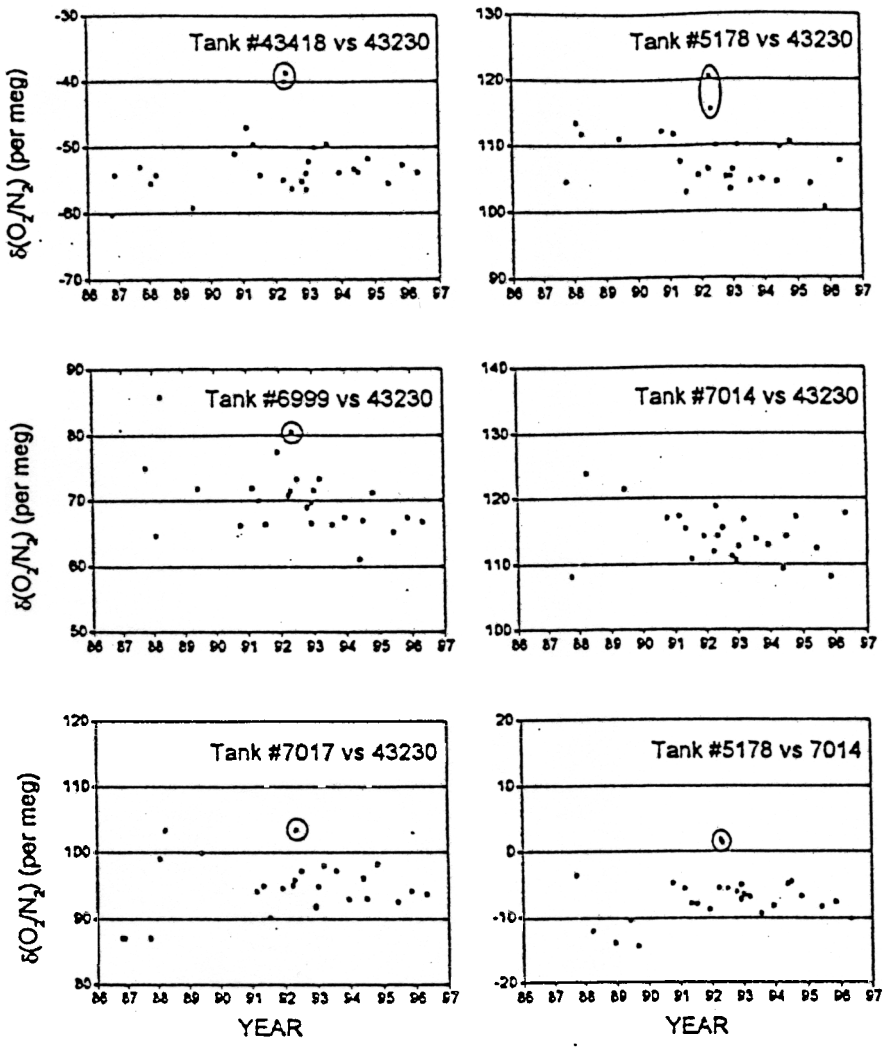

Figure 4. Differences in the O_2/N_2 ratios of the primary reference tanks. These comparisons began as early as 1986 before the procedure for determining the "S1" and "S2" scales was established. The circled squares correspond to comparisons made while the first tank of the pair was oriented horizontally within the insulated enclosure and the second tank was oriented upright on the laboratory floor. Before June 1992 all tanks were upright, and after this all tanks were horizontal in the enclosure. There are no circled squares for the pair 7014 versus 43230 because both tanks were relocated at the same time. Differences are not corrected for CO_2 interference (essentially constant in time).

the first 50 days, while the second is indicated by the continued decrease in O_2/N_2 accompanied by increases in CO_2 after 50 days. The second process is especially evident for the flasks with extra greased O-rings. We suspect that the first process involves the O-rings physically adsorbing O_2 (preferentially to N_2) and CO_2, and the second process involves oxidation of grease. Consistency between pairs is good, with the only exception being the long-term effects in the flasks containing greased O-rings. This discrepancy is most likely explained by the difficulty in reproducing accurately the amount of grease added to the extra O-rings and hence the degree of oxidation occurring in the flasks.

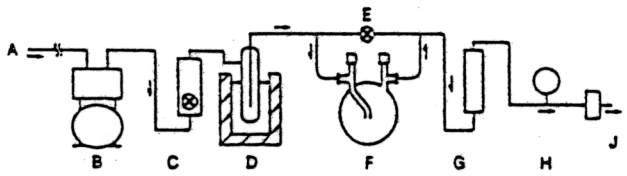

A INTAKE
B COMPRESSOR
C FLOWMETER WITH VALVE
D COLD TRAP
E BYPASS VALVE
F FLASK
G FLOWMETER
H PRESSURE GAUGE*
I BACKPRESSURE REGULATOR*
J EXHAUST

*USED ONLY AT HIGH ELEVATION

Figure 5. Apparatus used to collect samples in the field.

The "normal" flasks show excellent stability in O_2/N_2 from day 4 onward. Such stability is not inconsistent with the large variations that occurred in the flasks containing extra O-rings: we estimate that the total O-ring surface area exposed to the flasks was about 30 to 40 times greater in the flasks with extra O-rings, so drift rates were probably amplified by a similar factor. The normal flasks show a statistically significant upward drift of around 0.2 ppm CO_2 over the 313-day test period. We are not sure of the cause of this drift which appears

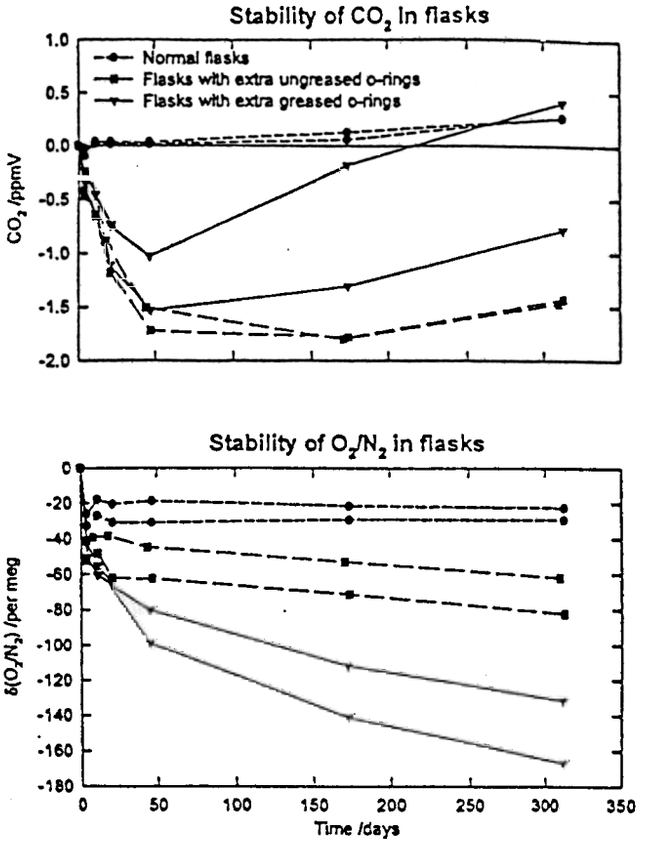

Figure 6. Concentration histories of flasks set aside for stability tests. Time is measured in days after the initial flushing. Concentrations are relative to the composition of the tank used for the flushing. The apparent drop in O_2/N_2 between day 0 and day 4 is likely spurious, arising not from changes in the flasks but due to changes in the composition of the air against which the flasks were measured.

somewhat too large to be explained by oxidation of grease when compared to the flasks with extra greased O-rings.

An important conclusion we can draw from these tests is that flasks that are properly preconditioned with dry air at atmospheric pressure can preserve air samples for times approaching 1 year at the level of a few per meg in O_2/N_2 and a few tenths of a ppm in CO_2.

5.4. Flask Reproducibility

Information on the inherent precision of our sampling and analysis procedures is contained in the reproducibility of the replicate flasks collected at a given time and site in our O_2 sampling network [*Keeling et al.*, 1998]. We have examined approximately 1500 replicate samples collected at seven sampling sites between 1989 and 1994. The only samples excluded from our analysis are those which were compromised by obvious procedural errors. We have computed the scaled residuals according to

$$d_i = (x_i - \bar{x})\sqrt{\frac{N}{N-1}} \qquad (5)$$

where x_i, $\bar{x}$, and N are the flask concentration (δ value for O_2/N_2 ratio, or mole fraction for CO_2), the replicate mean, and the number of replicates (typically 3), respectively. This scaling is used so that the residuals belonging to sets with different numbers of replicates (i.e., $N = 2,3,4,...$, etc.) all have the same standard deviation. This standard deviation is the same as that of the hypothetical parent distribution for large N.

Normal probability plots of the distribution of the scaled residuals for both O_2/N_2 and CO_2 are shown in Figure 7. The distributions include contributions from both sampling and analysis errors. Although these two forms of error cannot be rigorously distinguished with the available information, some clues are provided by the shape of the distribution.

The center of the O_2/N_2 distribution (Figure 7a) is nearly normal in shape (indicated by linearity on the plot), and we believe that this is a valid measure of the imprecision of our flask analyses. The standard deviation (1σ) implied by the center of the distribution for analysis of a single flask is ±3.3

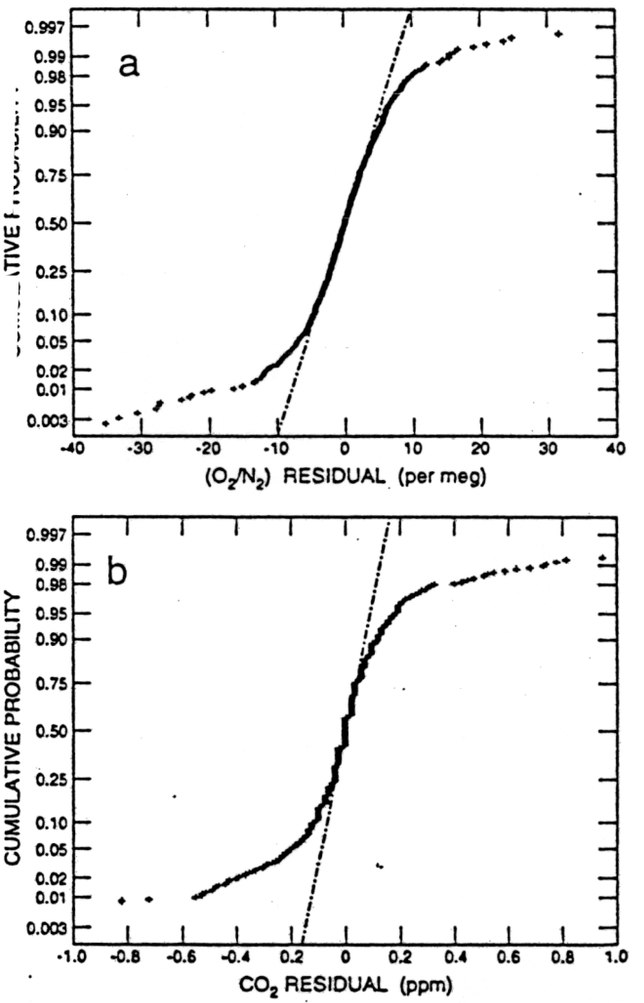

Figure 7. Cumulative probability of the O_2/N_2 residuals (a) and CO_2 residuals (b) versus the residuals. A normal probability distribution would yield a straight line on such a plot. The straight lines connect the 25% and 75% quantiles. The distributions are based on a total of 1413 and 1441 flask samples for O_2/N_2 and CO_2, respectively.

per meg. This is only slightly worse than the ultimate precision attainable from the interferometer considering that approximately five 30-s scans (each with a precision of ±5.4 per meg) are used to visually define the peak. With this interpretation the excess of larger residuals relative to this normal distribution is caused by real variations in the flask samples. Less than 10% of our flasks appear to be noticeably affected by such variations.

The situation is somewhat different for CO_2 where the distribution conforms less well to a Gaussian distribution. On the basis of the performance of the CO_2 analyzer we expect that analytical errors should be smaller than 0.05 ppm, so it is clear from Figure 7b that the residuals in CO_2 are dominated by real variations between flasks. The results indicate that the residuals are smaller than 0.2 ppm for 90% of our flasks.

6. Southern Hemisphere Air

We illustrate the geochemical application of our methods by comparing results from flask samples collected at three southern hemisphere stations: Cape Grim, Tasmania (40°41'S, 144°41'E, 94m) from 1991 to 1995, Macquarie Island (54°29'S, 158°58'E, 94m) from 1992 to 1994, and South Pole Station (89°59'S, 24°41'E, 2810m) from 1991 to 1995. Significant seasonal cycles are evident at all three stations, and the longer records at Cape Grim and the South Pole show significant interannual trends, as shown in Figure 8a. The data for Cape Grim and the South Pole are shown against curve fits based on the sum of a four-harmonic seasonal function and a stiff-spline interannual trend, where the spline stiffness is adjusted to suppress frequencies higher than about 1 year. To emphasize the interannual trends, the splines alone for these stations are shown in Figure 8b.

The seasonal cycles at Cape Grim and the South Pole are strikingly similar in spite of the large distance between these stations. These cycles are largely driven by O_2 and N_2 exchanges with the Southern Ocean, and the observed cycles have been shown to be consistent with reasonable source-sink distributions in the presence of atmospheric transport [*Keeling et al.*, 1996, 1998]. The seasonal cycle at Macquarie, although

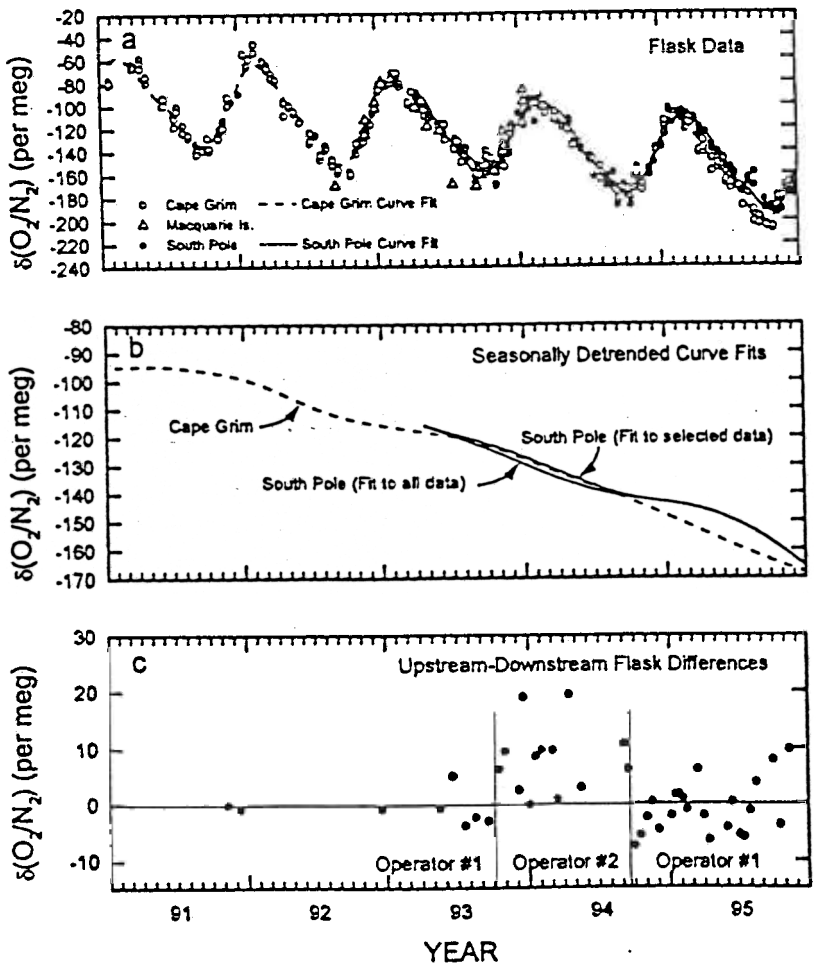

Figure 8. O_2/N_2 ratios observed in flasks sampled at Cape Grim and the South Pole. (a) Time series showing individual flask results and curve fits based on a four-harmonic seasonal cycle and a stiff-spline interannual trend. (b) Showing only the stiff-spline component to the trends. The South Pole curve has been derived both by including all data from 1993 to 1994 and also by including only flasks collected in the upstream position by operator 2 during 1993-1994. (c) Showing the differences in the O_2/N_2 ratios of flasks collected in the upstream and downstream positions. Note the tendency for positive differences during the period when operator 2 collected samples during 1993-1994.

based on more limited observations, appears slightly larger in amplitude than the cycles at the other two stations. There is weak evidence, based on the three samples collected during the months of July 1992, July 1993, and September 1993, that the seasonal minimum at Macquarie is deeper and occurs earlier in the year than the minimum at Cape Grim and the South Pole. Such a feature is expected considering that Macquarie Island is closer to the high-latitude regions of the Southern Ocean which comprise a large wintertime O_2 sink [*Najjar and Keeling*, 1997].

The long-term trend observed at Cape Grim is generally in good agreement with that observed at South Pole, as expected considering that large differences in concentration cannot build up indefinitely due to atmospheric mixing. Of particular interest is the apparently significant gradient observed between Cape Grim and the South Pole as revealed by the nonseasonal component of the trends in Figure 8b. The gradient appears to vary interannually, being smaller during a period in 1993-1994 than after that period. We have computed differences between the monthly concentrations at the South Pole and Cape Grim during months when both stations had observations. On the basis of 41 represented months between November 1991 and February 1996 we compute an average difference of 3.6 ±1.4 per meg, with higher values at the South Pole, where the uncertainty is the standard error based on the precision of the monthly values. Monthly values were computed by adjusting the individual observations to the 15th of the month by effectively "sliding" the data parallel to the combined (spline plus harmonic) fit and then computing the average of the adjusted observations. The precision of the monthly values was computed from the differences of the monthly averages relative to the combined fit. This method, which yields a monthly precision of ±5.5 per meg at the South Pole and ±6.7 per meg at Cape Grim, allows for both analysis errors and synoptic variability but not interannual variability.

Direct observations show that the surface waters south of about 55°S on average are undersaturated in dissolved O_2 [*Levitus*, 1992; *Najjar and Keeling*, 1997] due to upwelling of oxygen-depleted waters south of the Polar Front. This feature must be associated with net uptake of O_2 from the atmosphere, which should lead to a lowering of O_2/N_2 ratios on average at latitudes south of Cape Grim unless compensated by other processes. Fossil-fuel burning and land biotic exchanges can only have minimal influence on the O_2/N_2 gradient at these latitudes, which are remote from terrestrial ecosystems and industrial activities. Atmospheric transport calculations which account for oceanic O_2 and N_2 exchanges using ocean models, for the rectification of seasonal exchanges by seasonally varying atmospheric transport, and for the (much smaller) influence of gradients due to fossil-fuel burning [*Stephens et al.*, 1998] predict O_2/N_2 ratios lower by 3 to 7 per meg at South Pole Station than at Cape Grim, driven mostly by uptake of O_2 by the Southern Ocean. It is possible that the ocean models may overestimate oceanic O_2 uptake around Antarctica [*Stephens et al.*, 1997], although even a reduction in these fluxes would not change the sign of the predicted gradient unless compensated by additional processes. Thus the higher O_2/N_2 ratios that we observe at South Pole relative to Cape Grim are not easy to reconcile with current understanding of geochemical processes.

Sampling at South Pole Station presents several unusual difficulties including the need to store flasks in a very cold storage environment for up to 9 months before analysis because access to the station is restricted to warmer months. Also, the risk of flask leakage during sampling or subsequent storage is aggravated because ambient station pressure, typically ~680 mbar, is significantly lower than the internal flask pressure which is always maintained at 1 atmosphere.

Concerned that the gradient we observe may reflect sampling biases at the South Pole, we have scrutinized these data for any evidence of problems. For each flask we computed the residuals in the O_2/N_2 ratio relative to a smooth curve fit to the time series data and also relative to the average of all flasks on each sampling date. We checked to see if the residuals (computed both ways) correlated with imbalances between upstream and downstream sampling flows or with variations in flask pressures (both indicators of possible leaks) and if they correlated with the age of each flask since it was manufactured (indicator of possible conditioning problems on newer flasks) and found no significant relationships.

The flasks at the South Pole are flushed in series, and the differences between the flasks collected in the upstream and downstream positions are shown in Figure 8c. Interestingly, during a 1 year period (1993-1994) when a particular operator was collecting samples, we found that the upstream flasks were 7±2 per meg higher on average than the downstream flasks. This period roughly coincides with the period of reduced gradient between Cape Grim and South Pole Station (Figure 8b). Indeed, retaining only the upstream flasks during this period yields a slightly more stable gradient between Cape Grim and the South Pole throughout the 1993-1995 period, suggesting that the O_2/N_2 ratios of the downstream flasks may have been biased downward during this period. One possible cause of such a bias is temperature gradients in the sampling environment leading to fractionation by thermal diffusion. Although we have not confirmed this effect, it is important to note that correcting for the bias does not resolve the qualitative discrepancy between the expected and the observed latitudinal gradients because the correction is of the wrong sign and only applies for part of the record.

We are continuing to explore whether other artifacts might result in an upward bias in the results from South Pole Station. One possibility is that some flasks leaked through the failure of the O-rings on the stopcocks due to the low temperatures and pressures in the storage environment at South Pole. From 1991 to 1995, eight flasks were returned from the South Pole with pressures between 850 and 900 mbar. These pressures lie between the initial fill pressure (near 1000 mb) and the station pressure (typically ~680 mbar) thus indicating leakage. Several of these flasks had O_2/N_2 ratios that were anomalously high by as much as 150 per meg. This enrichment might be qualitatively explained by fractionation by Knudsen diffusion through small leaks around the flask O-rings, which may tend to fail intermittently at low temperatures. Although these eight flasks were not considered in the results in Figures 8a and

8b because they had obviously leaked, it is possible that flasks with unnoticeably small pressure losses nevertheless were also compromised by small amounts of leakage. To test if flasks are affected by such leakage, we have recently started capping the ball-joint fittings on flasks from the South Pole which should reduce any such effects.

To summarize our findings, the results from the South Pole, Macquarie Island, and Cape Grim reveal coarse features, including seasonal cycles and the overall long-term trends, which agree well with geochemical expectations, but also reveal a gradient between the latitudes of Cape Grim and the South Pole which, though very small, is nevertheless hard to explain. Interannual variability may be a significant source of uncertainty, but at no time during the 4 year period spanned by our observations have we found significantly lower values at the South Pole, as would have been expected from model predictions. If O_2/N_2 ratios are indeed higher on average at the South Pole than at Cape Grim, this may require the existence of geochemical or atmospheric processes that have not yet been characterized. We have found no evidence that this gradient is an artifact of our methods, although tests are still ongoing.

7. Summary

We have outlined gas-handling methods for collecting air samples for O_2 analysis and for calibrating these measurements against reference gases. The methods are guided by the need to avoid fractionation due to surface adsorption and diffusive separation in the presence of temperature, pressure, or humidity gradients. Fractionation is avoided by minimizing pressure and flow fluctuations during both sampling and analysis, which ensures that all surfaces are well conditioned with dry gas at constant pressure and that any volumes subject to diffusive fractionation are under conditions of steady flow.

The sampling methods are based on collecting samples in 5 L glass flasks with the air dried in the field. Flasks are collected indoors to minimize thermal gradients. We have shown that air samples can be collected and stored in such flasks for nearly 1 year with a stability of 2 to 3 per meg. The external reproducibility is approximately ±3.3 per meg, which is nearly as good as that allowed by the internal precision of the interferometric O_2 analyzer.

The calibration method relies on comparing air samples to reference gases stored in high-pressure aluminum tanks. We have found that it is possible to achieve short-term reproduciblity in O_2 concentrations from such tanks to the level of ±1.5 per meg if the following precautions are adopted: the tanks are stored horizontally in an insulated enclosure; pressure regulators and any surfaces exposed to high pressures are well conditioned at tank pressure before reference gas is delivered; and gas is delivered only under steady flow. Pressure-induced desorption effects on the delivered concentrations appear as small or smaller than ±5 per meg as the tanks are depleted. We have found no evidence of long-term trends in the relative concentrations in a suite of six primary reference tanks to the level of 5 per meg over a 9 year period.

The relative stability of our primary reference tanks suggests that these tanks are either all stable or are all drifting in the same direction at the same rate. We feel that the latter possibility is highly unlikely given that the tanks have different pressures and are different sizes (see Table 2). Nevertheless, to establish a firm long-term reference for O_2/N_2 measurements, references independent of air stored in high-pressure tanks are also needed.

We have illustrated the results of our method for air samples collected at Cape Grim, (41°S), Macquarie Island (54°S), and South Pole Station (90°S). The results indicate that the seasonal cycle at Macquarie Island may have a larger amplitude and an earlier minimum than the other two stations. The results from Cape Grim and South Pole indicate that a small and variable gradient in the O_2/N_2 ratio exists between the stations, with generally higher values at South Pole. This gradient is hard to explain considering that the Southern Ocean is expected to be an important sink for O_2. Concerned that this difference may reflect sampling problems at the South Pole, we have scrutinized these data for evidence of possible systematic effects. To date we have found no artifacts that could bias South Pole data upward, although tests are still ongoing. These data illustrate the extreme care which may be required to recover signals of biogeochemical significance. The higher concentrations at South Pole may require unexpected sources of O_2 around or over Antarctica or unexpected atmospheric transport patterns.

Appendix A: Interferometric O_2 Analyzer

Oxygen concentrations are determined in our laboratory by the interferometric method, based on detecting changes in relative refractivity, given by

$$r(\lambda_1,\lambda_2) = \frac{n(\lambda_1) - 1}{n(\lambda_2) - 1} \qquad (6)$$

where $n(\lambda)$ is the refractive index at vacuum wavelength λ. Here λ_1 and λ_2 are the 2537.2688 Å and 4358.5662 Å lines of ^{198}Hg, respectively [see *Kaufman*, 1962]. The relative refractivity can be expressed as a linear function of composition according to eq (2), where the sensitivity factors S_i are expressed according to

$$S_i = \left(\frac{n_i(\lambda_2)-1}{n_{air}(\lambda_1)-1}\right)\left(\frac{r_i(\lambda_1,\lambda_2)-r_{air}(\lambda_1,\lambda_2)}{1 - X_i}\right) \qquad (7)$$

where $n_i(\lambda)-1$ and $r_i(\lambda_1,\lambda_2)$ are the refractivity (at standard pressure and temperature) and relative refractivity of constituent i, respectively [*Keeling*, 1988b].

The refractivity data, sensitivity coefficients, and the (arbitrary) reference concentrations, used for correcting for the effects of trace gases on the relative refractivity, are summarized in Table 3. We now use a sensitivity coefficient for O_2 based on our own recent measurements of the O_2 relative refractivity. The new sensitivity coefficient is 7% larger than the coefficient used in publications prior to 1996 [*Keeling*, 1989b; *Keeling and Shertz*, 1992].

Table 3. Refractivity Data and Sensitivity Coefficients

Gas	Reference Abundance, ppm	Relative Refractivity, $\frac{n(2537)-1}{n(4359)-1}$	Refractivity[a] at 0°C, 760 torr $(n(4359)-1)\times 10^4$	Sensitivity Coefficient $S_i \times 10^8$, ppm^{-1}
Dry Air		1.06901[a]	2.965[b]	
O_2		1.09792[c]	2.754[b]	3.320
CO_2	363.29	1.07300[a]	4.562[b]	0.614
CH_4	1.5	1.09349[a]	4.513[b]	3.73
H_2	0.5	1.0912[b]	1.417[b]	1.06
N_2O	0.3	1.09920[a]	5.138[b]	5.23
CO	0.0	1.10533[a]	3.418[b]	4.19

[a]From measurements reported in Appendix B of *Keeling* [1988a].
[b]References given by *Keeling* [1988b], Table 1.
[c]From relative refractivity measurements performed on the interferometer shown in Figure 9 using procedures described in Appendix B of *Keeling* [1988a]. These measurements used O_2 with a certified purity of 99.9999%.

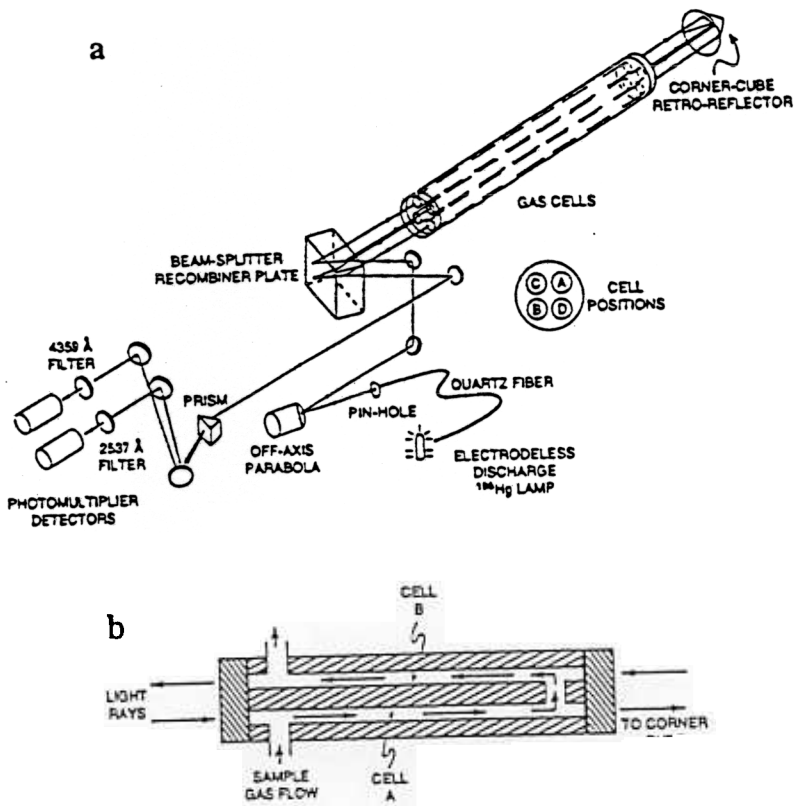

Figure 9. Optical interferometer used for O_2/N_2 measurements. (a) Optical design. Emission from the ^{198}Hg lamp is collimated by the pinhole and off-axis parabola and directed onto the partially reflecting front face of the beam-splitter/recombiner plate, where it is divided into two beams. Each of these beams traverses two coupled gas cells, one beam traversing cells A and B and the other cells C and D. The beams are recombined on the beam-splitter/recombiner plate, and the resulting combined beam is then separated spectrally by a prism, and the two used spectral lines are spectrally further isolated by interference filters and detected by photomultiplier tubes. (b) Sample flow path. Air samples flow through cells A and B as shown. Cells C and D, which are similarly connected, are used only to modulate the fringe positions. This is done by bleeding dry compressed air into cells C and D from less than 0.1 kPa to 1.6 kPa and recording the temporally varying photomultiplier signals. These signals are then processed numerically to compute ϵ [see *Keeling*, 1988a]. These pressure scans are repeated at 30 s intervals.

The interferometer used for the relative refractivity measurements is shown schematically in Figure 9. The measurement is based on changes in the relative positions of interference fringes at two mercury wavelengths [*Keeling*, 1988a, b]:

$$\delta r = \frac{\lambda_1}{\lambda_2} \frac{\delta \epsilon}{\mathrm{OPD}} \tag{8}$$

Here $\delta\epsilon$ is the change in relative position of a particular adjacent pair of 2537Å and 4359Å fringes, expressed in units of a 2537Å fringe, and where OPD is the optical path difference (in units of 4359Å fringes) between the two arms of the interferometer caused by the air sample being in one arm. The quantity ϵ is determined every 30 s with a short-term precision of approximately ±0.0002, which for typical operating conditions corresponds to ±5.4 per meg. Typical operating characteristics are summarized in Table 4. Details are described elsewhere [*Keeling*, 1988a].

The span sensitivity of the interferometric O_2 analyzer depends on the relative refractivity sensitivity coefficients in eq (7) and on the factors in eq (8). The sensitivity coefficients are essentially fixed constants highly insensitive to temperature and pressure [*Keeling*, 1988a]. The only variable factor in eq (8) is OPD, which is a measure of the number of fringes that elapse when the sample cell is filled from vacuum to operating pressure and is proportional to the path length of the interferometer multiplied by the refractivity, which is proportional to the sample density. Because the path length of the interferometer is constant, we determine OPD on a daily basis from sample pressure (gage *z* in Figure 1) and temperature. The sample pressure gage is intermittently calibrated against OPD by directly filling the cell from vacuum and counting fringes while simultaneously recording the sample pressure and temperature.

Appendix B: CO_2 Calibration Methods

Our CO_2 measurements are calibrated using procedures analogous to those used for O_2/N_2 ratios. The same pair of secondary reference gases used for the O_2/N_2 measurements are prepared with CO_2 concentrations that span ambient concentrations, and on the basis of these two tanks, we create a preliminary ("S1") scale for CO_2 which is linear in analyzer response. Corrections to this "S1" scale are assessed from analyses of six different primary reference gases that span a range from 301 to 419 ppm and that have been analyzed against the manometric scale maintained at the CO_2 laboratory of C. D. Keeling at the Scripps Institution of Oceanography. These primaries are measured periodically on the "S1" scale in an analogous fashion to the O_2 primaries, and this scale is then adjusted to bring the primaries in line with the manometric scale. The corrections take the form of a time-dependent cubic function of the "S1" scale reading. The corrected "S1" values are referred to as the "S2" values.

Table 4. Interferometer Specifications and Operating Conditions

Sample cell length (one way)	133.82 cm
Cell inner diameter	1.27 cm
Sample cell volume (cell A + cell B)*	~360 cm^3
Typical sample-cell pressure	237 kPa
Typical sample-cell temperature	21°C
Typical sample flow rate	4.7 STP cm^3 s^{-1}
Typical optical path difference, OPD(λ_2)	3934

*See Figure 9.

The dilution factors for the flask analyses are determined for CO_2 using the same methods as for O_2. The CO_2 dilution factor varies between 0.965 and 0.99 for flask pressures between 920 and 1090 mbar. The dilution factor for CO_2 is closer to unity than that for O_2 because the CO_2 analyzer cell is closer to the flask and smaller in volume than the interferometer cell. Thus the CO_2 cell is more nearly filled with pure flask air at the sweep-out "peak."

Acknowledgments. We thank Roger Francey of CSIRO Australia, staff at the Cape Grim Baseline Station, staff of the Australian Bureau of Meteorology at Macquarie Island, and staff of the NOAA-CMDL program at the South Pole for collection of air samples, and we thank Bill Paplawsky and Chris Atwood for assistance in the laboratory analyses. The manuscript was improved by helpful comments from two anonymous reviewers. The O_2 measurement program at Scripps has been supported by the National Science Foundation under grants ATM-9309765 and ATM-9612518 and by the Environmental Protection Agency Global Change Research Program under IAG DW49935603-01-2.

References

Bender, M. L., P.P.Tans, J.T. Ellis, J. Orchardo, and K. Habfast, High precision isotope ratio mass spectrometry method for measuring the O_2/N_2 ratio of air, *Geochim.Cosmochim.Acta, 58*, 4751-4758, 1994.

Bender, M., J.T. Ellis, P.P. Tans, R.J. Francey, and D. Lowe, Variability in the O_2/N_2 ratio of southern hemisphere air, 1991-1994: Implications for the carbon cycle, *Global Biogeochem. Cycles, 10*, 9-21, 1996.

Chapman, S., and T.G. Cowling, *The Mathematical Theory of Non-Uniform Gases*, 423pp., Cambridge Math. Libr., 1970.

Dushman, S., *Scientific Foundations of Vacuum Technique*, 806pp., John Wiley, 1962.

Grew, K.E., and L.T. Ibbs, *Thermal Diffusion in Gases*, 143 pp., Cambridge Univ. Press, New York, 1952.

Kaufman, V., Wavelengths, energy levels, and pressure shifts in mercury 198, *J.Opt.Soc.Am., 52*, 866-870, 1962.

Keeling, R.F.,*Development of an interferometric oxygen analyzer*, Ph. D. thesis, 178pp., Harvard Univ., Cambridge, Mass., 1988a.

Keeling, R.F.,Measuring correlations between atmospheric oxygen and carbon dioxide mole fractions: a preliminary study in urban air, *J. Atmos. Chem., 7*, 153-176, 1988b.

Keeling, R.F., and S.R. Shertz, Seasonal and interannual variations in atmospheric oxygen and implications for the global carbon cycle, *Nature, 358*, 723-727, 1992.

Keeling, R.F., R.G. Najjar, M. L. Bender, and P.P Tans, What atmospheric oxygen measurements can tell us about the global carbon cycle, *Global Biogeochem. Cycles, 7*, 37-67, 1993.

Keeling, R.F., S.C. Piper, and M. Heimann, Global and hemispheric CO_2 sinks deduced from changes in atmospheric O_2 concentration, *Nature, 318*, 218-221, 1996.

Keeling, R.F., B.B. Stephens, R.G. Najjar, S.C. Doney, D. Archer, and M. Heimann, Seasonal variation in the atmospheric O_2/N_2 ratio in relation to the kinetics of air-sea gas exchange, *Global Biogeochem. Cycles*, in press, 1998.

Levitus, S., Climatological atlas of the world ocean, *NOAA Prof. Pap. 13*, U.S. Dep. of Comm., Washington, D.C., 1982.

Machta, L., E. Hughes, Atmospheric Oxygen in 1967 to 1970, Science, *168*, 1582-1584, 1970.

Najjar, R. G., and R. F. Keeling, Analysis of the mean annual cycle of the dissolved oxygen anomaly in the world ocean, J. Mar. Res., *55*, 117-151, 1997.

Severinghaus, J.P., M.L. Bender, R.F. Keeling, and W.S. Broecker, Fractionation of soil gases by diffusion of water vapor, gravitational settling, and thermal diffusion, *Geochim.Cosmochim.Acta*, *60*, 1005-1018, 1996.

Stephens, B.B., R.F. Keeling, M. Heimann, K.D. Six, R. Murnane, K.Caldiera, Testing global ocean carbon cycle models using measurements of atmospheric O_2 and CO_2 concentration, *Global Biogeochem. Cycles*, in press, 1998.

R.F. Keeling, A.C. Manning, and E.M. McEvoy, Scripps Institution of Oceanography, University of California, San Diego, La Jolla, CA 92093-0236. (e-mail: rkeeling@ucsd.edu; andrew@ucsd.edu, emcevoy@ucsd.edu)

S.R. Shertz, National Center for Atmospheric Research, 1850 Table Mesa Dr., Bounder, CO 80303. (e-mail: shertz@ucar.edu)

(Received April 29, 1997; revised September 3, 1997; accepted September 4, 1997)